Cascade Reconstruction at the Glashow Resonance in IceCube

THE ICECUBE COLLABORATION[1]

[1] *See special section in these proceedings*

joanna.kiryluk@stonybrook.edu

Abstract: IceCube is a cubic kilometer neutrino detector located at the South Pole. Observation of the spectrum near the characteristic energy $E_\nu \simeq 6.3\,\mathrm{PeV}$ of the Glashow resonance, the interaction of anti-neutrinos with atomic electrons via $\bar{\nu}_e + e^- \to W^-$, is of particular interest, since it offers the unique possibility to determine the contribution from electron anti-neutrinos to the diffuse flux of astrophysical neutrinos. The flux of electron anti-neutrinos, if observed, provides new constraints on the possible production mechanisms for high-energy neutrinos in astrophysical sources. The dominant signatures of neutrino interactions at the Glashow resonance are particle showers (cascades), originating from hadronic W^- decay. The corresponding signal is anticipated to exceed the continuum of deep-inelastic-scattering induced cascades by up to a factor of 10. Assuming an extraterrestrial electron neutrino flux $E^2\Phi = 1 \times 10^{-8}\,\mathrm{GeV \cdot cm^{-2} \cdot s^{-1} \cdot sr^{-1}}$ and a neutrino to anti-neutrino ratio of $(\nu_e : \bar{\nu}_e) = (1:1)$, which is a generic prediction for pure proton-proton (pp) sources, we expect to detect 0.9 events per year that are contained within the instrumented volume of IceCube.

Corresponding authors: J. Kiryluk[2] and H. Niederhausen[2]
[2]*Department of Physics and Astronomy, Stony Brook University, Stony Brook NY 11794-3800*

Keywords: Glashow resonance, IceCube, Cascades, Reconstruction

1 Introduction

IceCube is a cubic-kilometer neutrino detector at the South Pole [1]. IceCube's primary science goal is the discovery and study of high energy extraterrestrial neutrinos of all flavors. IceCube detects neutrinos indirectly, typically through deep inelastic scattering (DIS) off the nucleons in the ice. Electron anti-neutrinos of $E_\nu \sim 6.3\,\mathrm{PeV}$ have an enhanced probability to scatter off atomic electrons in the ice by forming an on-shell W^--boson, the so-called Glashow resonance (GR) [2]. The GR events can be used to quantify the contribution of $\bar{\nu}_e$ to the electron neutrino flux $\Phi_{\nu_e + \bar{\nu}_e}$ at earth, which mainly relates to the ratio between the abundances of charged pions (π^-, π^+) at source region. For purely hadronic pp sources, $(\nu_e : \bar{\nu}_e) \approx (1:1)$ while $(\nu_e : \bar{\nu}_e) \approx (1:0)$ for purely photo hadronic pγ sources [3]. Assuming tribimaximal neutrino mixing[1], this relates to the following electron type neutrino flux composition at earth: $(\nu_e : \bar{\nu}_e) \approx (1:1)$ for pp sources and $(\nu_e : \bar{\nu}_e) \approx (0.78 : 0.22)$ for pγ sources [3].

2 Glashow Resonance: Cascade Channel

The W^- produced in $\bar{\nu}_e + e^-$ interaction decays predominantly into a hadronic particle shower with a combined branching ratio of $\Gamma_\mathrm{hadr}/\Gamma_{tot} = 0.68$. The W^- decay modes into a charged lepton and the corresponding anti-neutrino have a branching ratio of $\Gamma_{l\bar{\nu}_l}/\Gamma_{tot} = 0.11$ [6]. Thus, the fraction of W^- decays that produces final state muons and the associated track-like signature is small and a search for resonance events is most promising in the cascade detection channel. Cascades from particle showers produce a nearly spherical light pattern in the IceCube detector, as illustrated in Fig. 1 which shows a simulated GR hadronic cascade event. Cascades offer superior accuracy in energy measurement compared to muon tracks, which deposit only a fraction of their energy in the detector. With the recent obser-
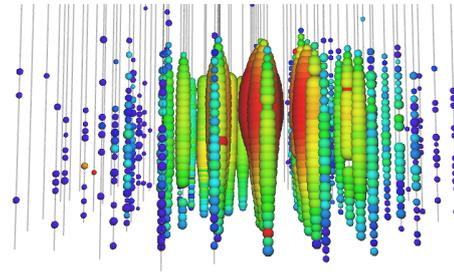

Fig. 1: Event display for a simulated Glashow resonance hadronic cascade, $\bar{\nu}_e + e^- \to W^- \to$ hadrons for the IceCube 79-string detector configuration.

vation of two ~ 1 PeV cascades [7], IceCube has already begun to explore the interesting high energy range that will eventually extend to the energy of the Glashow resonance peak.

Figure 2 shows the expected neutrino primary spectra for pp sources (top) and pγ sources (bottom) for an assumed isotropic electron (anti-) neutrino flux of $E^2\Phi = 1 \times 10^{-8}\,\mathrm{GeV \cdot cm^{-2} \cdot s^{-1} \cdot sr^{-1}}$ at the Earth as obtained from Monte Carlo simulations for the IceCube 79-string detector configuration (IC79). The GR events (red: hadr., pink: $e^- \bar{\nu}_e$) exceed the continuum of DIS induced cascades (blue: Charged Current CC events, green: Neutral Current NC events) around $E_\nu = 6.3\,\mathrm{PeV}$. In this figure we require the events to pass the online cascade filter [8], which is designed to select events with almost spherical light deposition. Furthermore, we require that all events develop their associated shower maxima, where most of the Cherenkov photons are emitted, within the fiducial volume of IceCube.

---

1. Now ruled out because θ_{13} is large [4, 5].
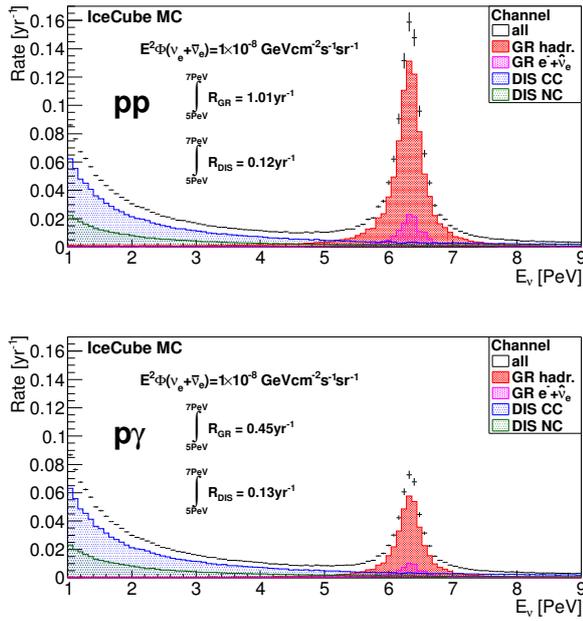
Fig. 2: Anticipated electron (anti)neutrino interaction rates in the IceCube 79-string detector configuration versus true Monte Carlo electron anti-neutrino energy E_ν for pure pp (top) and pure pγ (bottom) sources. All events are required to pass the IceCube online cascade selection filtering and shower containment criteria.
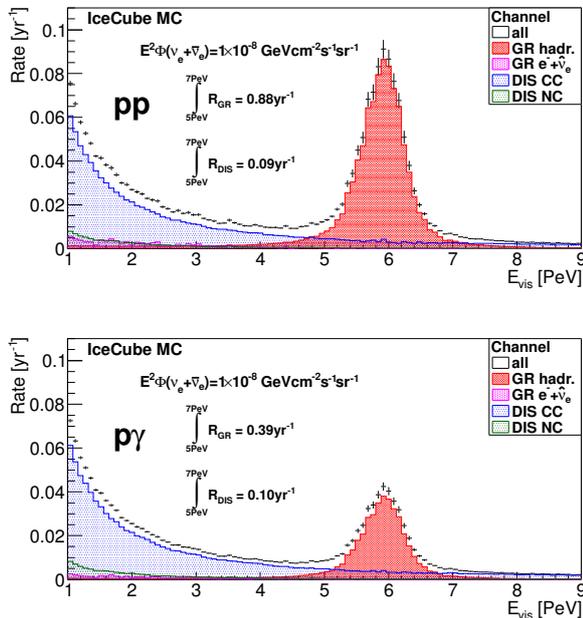
Fig. 3: Electron (anti)neutrino interaction rates in IceCube 79-string detector configuration versus true Monte Carlo visible cascade energy deposit, E_{vis}, expected from pure pp (top) and pure pγ (bottom) sources. All events are required to pass IceCube online cascade selection filtering criteria, as well as the shower containment criteria.

For pure pp sources we expect to observe 1.0 GR cascades per year induced by electron anti-neutrinos with en-

ergies between 5 PeV and 7 PeV. Due to the suppressed electron anti-neutrino contribution in the case of pure pγ sources this expectation is lowered to 0.5 events pear year while the DIS expectation remains stable at 0.1 events in the same neutrino energy range. On the other hand, processes like multiple-pion production can increase the expected anti-neutrino contribution at the source region by up to 20% [9] while muon cooling could almost completely suppress any electron anti-neutrino flux [10]. Corrections due to the recently established finite value of θ_{13} [4, 5] remain to be evaluated.

IceCube determines the neutrino energy from the "visible" energy E_{vis}, defined as the energy deposit of a purely electromagnetic cascade that produces the observed Cherenkov light yield. Figure 3 shows the distribution of the visible energy E_{vis} for the cases of pure pp and pure pγ sources. Due to hadronic physics in the $W^- \to q\bar{q}$ channel we expect to observe the resonant peak at slightly lower energies ($\sim 7\%$) compared to the neutrino spectrum shown in Fig. 2) and with a marginally larger width due to fluctuations in the Cherenkov light yield of hadronic cascades ($\sim 4\%$). Because of final state kinematics in the $W^- \to e^- + \bar{\nu}_e$ mode involving a neutrino with "invisible" energy, this channel does not contribute to the peak region of the GR, $5\,\text{PeV} < E_{vis} < 7\,\text{PeV}$, thus lowering the signal expectation by $\sim 10\%$ to 0.9 events per year. Measurement of the flux in the $5\,\text{PeV} < E_{vis} < 7\,\text{PeV}$ energy range is expected to provide insight in and constraints on the physics of cosmic ray accelerators.
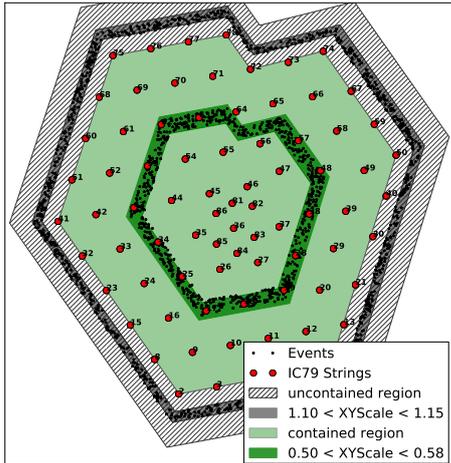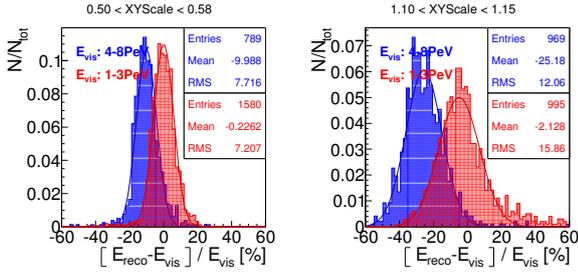
3 Cascade Reconstruction

Events with a cascade topology are described by a set of seven parameters $C_0 = \{E_{vis}, \vec{x}_{vis}, t_0, \theta_0, \phi_0\}$ assuming point-like Cherenkov emission. Here, $\vec{x}_{vis}, t_0$ denote the position of the shower maximum and the corresponding time, and θ_0 and ϕ_0 the orientation of the shower axis, the neutrino arrival direction. We obtain the values for these parameters by matching the photon arrival time distributions measured in each photomultiplier tube to the expectation for a hypothetical cascade characterized by known parameter values C_h. The expected probability density functions (pdfs) corresponding to C_h are obtained from Photonics simulation [11]. The matching is done by using a Poisson likelihood technique [12].

4 Performance on simulated GR Cascades

In order to estimate the accuracy of the reconstruction method we rely on simulations of neutrino interactions, Cherenkov light emission and propagation, and detector response.

The same processing and filtering was applied to simulated events as to the data recorded with the IceCube 79-string configuration at the South Pole.
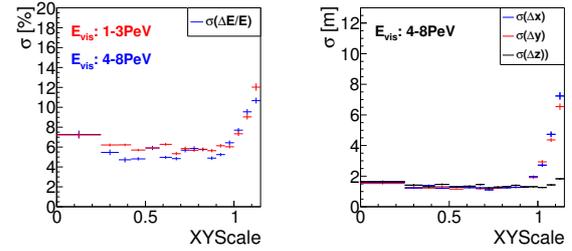
In this analysis we use only hadronic GR cascades that satisfy the following selection criteria: $1\,\text{PeV} < E_{vis} < 10\,\text{PeV}$ and $(-350\,\text{m} < Z_{vis} < -200\,\text{m}$ or $100\,\text{m} < Z_{vis} < 350\,\text{m})$. The former ensures that the events cover the energy range of interest while the latter ensures that the showers do not lose significant fractions of their energy in the known dust layer within the detection volume or in regions below and above the detector. The level of the shower containment for the analyzed samples is controlled in the xy-plane by

Fig. 5: Electron neutrino Monte Carlo. Resolution of the reconstructed energy (left) and of the reconstructed vertex (right) as a function of the detector containment variable XYScale.


Fig. 4: Top: the distribution of $(E_{redo} - E_{vis})/E_{vis}[\%]$ in the energy range $1\,\text{PeV} < E_{vis} < 3\,\text{PeV}$ (red histogram) and $4\,\text{PeV} < E_{vis} < 8\,\text{PeV}$ (blue histogram) for contained events (left) and partially contained events (right) from electron-neutrino Monte Carlo simulation. Bottom: the corresponding location of the shower maximum in x and y.

using the detector scaling variable (XYScale). The XYScale value depends on the position of the shower maximum in the xy-plane, and XYScale = 1 specifies the set of points defined by the polygon of the outermost layer of IceCube strings. This polygon then scales linearly in that variable; XYScale < 1 implies that the event develops its shower maximum within the instrumented region of IceCube, as illustrated in Fig. 4 (bottom).

Figure 4 (top) shows the distributions of the difference between the reconstructed visible energy and the MC truth relative to the MC true visible energy for contained showers with $0.50 < $XYScale$ < 0.58$ (left) and partially contained showers with $1.10 < $XYScale$ < 1.15$ (right) in two energy bins: $1\,\text{PeV} < E_{vis} < 3\,\text{PeV}$ (red histogram) and $4\,\text{PeV} < E_{vis} < 8\,\text{PeV}$ (blue histogram). Figure 5 shows the resolution ($\sigma_{\Delta E}$) of the energy reconstruction as determined from the parameters of a gaussian fit to the relative differences in Fig. 4 (top) for different XYScale values. Within the detection volume we achieve an energy resolution of $5-8\%$ for GR cascades which is sufficient to observe the (anticipated) GR signal above the DIS continuum at PeV energies. For partially contained cascades ($1.0 < $XYScale$ < 1.15$) we find better than 15% energy resolution. The MC simulations show that the reconstructed energies in the $4\,\text{PeV} < E_{vis} < 8\,\text{PeV}$ bin are underestimated by $\sim 10\%\,(25\%)$ for fully (partially) contained

cascades. This effect is not observed in the lower energy bin $1\,\text{PeV} < E_{vis} < 3\,\text{PeV}$. Further studies are needed. The inclusion of partially contained cascades in the analyzed sample can enhance our expected GR signal rate by up to $\sim 50\%$.

Figure 5 quantifies how well the position of the shower maximum of the GR signal cascades is resolved. The results were obtained from the parameters of a gaussian fit to the difference between true and reconstructed x,y and z positions. No bias is found in the vertex reconstruction. The vertex resolutions along each of the three coordinates within the detection volume is about 1.5 m. While the z-position of the shower is still well constrained beyond the detection volume with an accuracy of better than 2 m up to XYScale = 1.15, the resolution in x and y quickly worsens by a factor of up to five. This is due to the difference in spacing between adjacent detector elements in these coordinates.

The zenith angle θ is of interest in the reconstruction of the cascade direction, as is the opening angle Ψ between the true and reconstructed cascade direction. For contained events (XYScale< 0.95) we find a median angular (zenith) resolution $\theta_{0.5} = \text{Median}\{|\theta_{reco} - \theta_0|\}$ of $\sim 5°$ and a median directional resolution $\Psi_{0.5} = \text{Median}\{|\Psi|\}$ of $\sim 8°$. The median zenith resolution is $\theta_{0.5} \simeq 9°$ for uncontained cascades with $0.95 <$XYScale< 1.15, and the median directional resolution is $\Psi_{0.5}$ between $8°$ and $27°$.

5 Performance on laser data

In order to verify the cascade reconstruction performance independent from Monte Carlo simulation, we analyzed calibration laser data recorded with the 79-string detector configuration in 2011. This nitrogen laser, deployed in clear ice at a depth of 2153 m, emits photons at the near-UV wavelength of 337 nm and its light deposition mimics the point like light pattern of highly energetic cascades. A reflective cone ensures that photons are emitted at the Cherenkov angle of 41°. Different attenuation filters make it possible to adjust the laser brightness. In this study we reconstructed 1000 laser flashes for each of the three brightness levels (1.6%, 3.2% and 8.9% of the maximum brightness) that cover the PeV energy region of interest for this analysis. Figure 6 (top) shows the distribution of the fractional deviation of the reconstructed energy E_{reco} from the mean reconstructed energy E_{reco}^{mean} for the lowest (left) and highest (right) laser brightness used in this analysis. We find excellent energy resolutions of better than 2% for
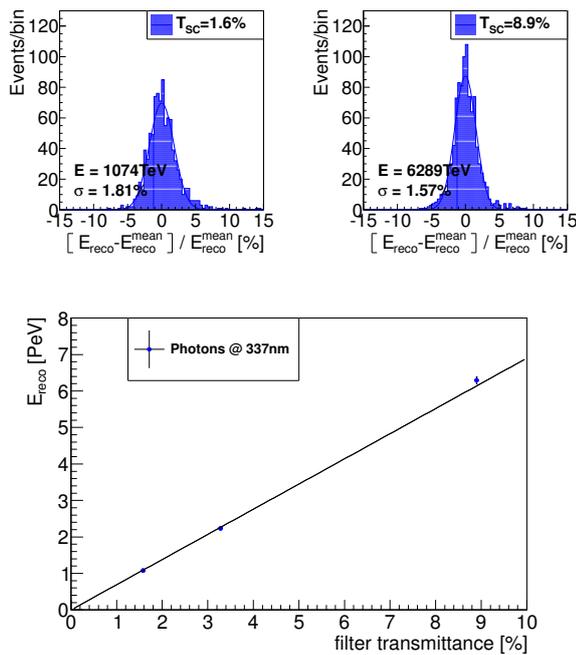
Fig. 6: Top: the fractional deviation of the reconstructed energy E_{reco} from the mean reconstructed energy E_{reco}^{mean} for the 1.6% laser transmittance (left) and the 9% filter transmittance (right). Bottom: best fit reconstructed energy values [PeV] versus filter transmittance [%] .

these events. This result is comparable to the per-pulse fluctuations of the laser brightness, which were found to be less than 3% in laboratory measurements before its deployment at the South Pole. The best-fit energies range from 1.1 PeV to 6.3 PeV. In Fig. 6 (bottom) the dependence of the best-fit values and their statistical uncertainties is shown as a function of the filter transmittance (laser brightness). The three data points are well described by a one-parameter linear fit, as expected in view of the linearity of the device. In addition, we found that the vertex resolutions are better than 0.35 m in x and y, independent of the laser brightness for filter transmittance settings between 1.6% and 9%. We observe a systematic shift of the best-fit value from the known laser position of up to 0.80 m. This may be due to systematic uncertainties associated with the description in the analysis of the in-ice light propagation at a wavelength of 337 nm, which is obtained by extrapolation from the ice properties (scattering and absorption lengths) determined using the LED calibration system at 400 nm [13].

6 Summary

One of the primary goals of IceCube is to observe the flux of high-energy cosmic neutrinos and anti-neutrinos from astrophysical sources. The (anti-)neutrino spectrum near the characteristic energy $E \sim 6.3$ PeV of the Glashow resonance offers the unique possibility to determine the contribution from electron anti-neutrinos and provides new constraints on the possible production mechanisms for high-energy (anti-)neutrinos in astrophysical sources. The dominant signatures of neutrino interactions at the Glashow

resonance in IceCube are particle showers, originating from hadronic W^- decay with a combined branching ratio of 70%. Assuming a neutrino to anti-neutrino ratio of $(\nu_e : \bar{\nu}_e) = (1 : 1)$, which is a generic prediction for pure pp sources, we expect the integrated GR signal rate to be an order of magnitude larger than its DIS counterpart in the 5 PeV to 7 PeV energy range. The GR signal is less pronounced in the case of pure pγ sources, but is still anticipated to be four times larger than the DIS contribution. Assuming an extraterrestrial electron type neutrino flux of $E^2\Phi = 1 \times 10^{-8}$ GeV $\cdot$ cm$^{-2} \cdot$ s$^{-1} \cdot$ sr^{-1} that is based purely on pp (pγ) collisions we expect to detect $0.9\,(0.4)$ GR signal cascade events per year that are contained within the instrumented volume of IceCube.

For fully contained GR cascades we expect to reconstruct the energy E_{vis} with a resolution of 5% to 8%, not including systematic uncertainties. Even in the region beyond the outermost IceCube strings with XYScale < 1.15 we obtain useable energy resolutions of better than 15%. Including this region into a future GR analysis of data is simulated to increase our expected signal rates by up to $\sim 50\%$.

We have verified our simulation methods using experimental data obtained by pulsing an in-situ calibration laser at three different brightness settings, corresponding to the energy range of 1.1 PeV $< E_{reco} < 6.3$ PeV. We find energy resolutions of better than 2% for these data. Within statistical uncertainties, the best-fit energies increase linearly with the laser intensity.

We conclude that IceCube has the capability to resolve a GR signal above the DIS continuum. The recent observation of two ~ 1 PeV cascades in IceCube indicates that a flux may exist.

References

[1] A. Achterberg *et al.*, Astropart. Phys. 26 (2006) 155-173 doi:10.1016/j.astropartphys.2006.06.007.

[2] S. L. Glashow, Phys. Rev. 118 (1960) 316-317 doi:10.1103/PhysRev.118.316.

[3] A. Bhattacharya *et al.*, J. Cosmol. Astropart. Phys. 10 (2011) 017 doi:10.1088/1475-7516/2011/10/017.

[4] F. P. An *et al.*, Phys. Rev. Lett. 108 (2012) 171803 doi:10.1103/PhysRevLett.108.171803.

[5] J. K. Ahn *et al.*, Phys. Rev. Lett. 108 (2012) 191802 doi:10.1103/PhysRevLett.108.191802.

[6] J. Beringer *et al.*, Phys. Rev. D86 (2012) 010001 doi:10.1103/PhysRevD.86.010001.

[7] M. G. Aartsen *et al.*, arXiv:1304.5356 [astro-ph.HE] (2013).

[8] M. Lesiak-Bzdak and A. Stoessl (for the IceCube Collaboration), paper 0697 these proceedings.

[9] W. Winter, Advances in High Energy Physics 2012 (2012) 586413 doi:10.1155/2012/586413.

[10] T. Kashti *et. al.*, Phys. Rev. Lett. 95 (2005) 181101 doi:10.1103/PhysRevLett.95.181101.

[11] J. Lundberg *et al.*, Nucl. Instr. Meth. Phys. Res. A 581 (2007) 619 doi:10.1016/j.nima.2007.07.143.

[12] E. Middell *et al.*, (for the IceCube Collaboration), Proceedings of the 31st ICRC (2009), paper 0708.

[13] M. G. Aartsen *et al.*, Nucl. Instr. Meth. Phys. Res. A 711 (2013) 73, doi:10.1016/j.nima.2013.01.054.